Hydrobiologia (2018) 806:47–65
https://doi.org/10.1007/s10750-017-3333-x

PRIMARY RESEARCH PAPER

Native and non-native halophytes resiliency against sea-level rise and saltwater intrusion

Lian Xue · Xiuzhen Li · Zhongzheng Yan · Qian Zhang · Wenhui Ding · Xing Huang · Bo Tian · Zhenming Ge · Qiuxiao Yin

Received: 9 September 2016 / Revised: 28 June 2017 / Accepted: 31 July 2017 / Published online: 9 August 2017

Abstract We quantified the independent impacts of flooding salinity, flooding depth, and flooding frequency on the native species, *Phragmites australis* and *Scirpus mariqueter*, and on the invasive species *Spartina alterniflora* in the Yangtze River Estuary, China. Total biomass of all three species decreased significantly with increasing salinity, but *S. alterniflora* was less severely affected than *P. australis* and *S. mariqueter*. Elevated flooding depth significantly decreased their live aboveground biomass of *P. australis* and *S. mariqueter*, while *S. alterniflora* still had high live aboveground biomass and total biomass even at the highest flooding depth. These findings indicated that *S. alterniflora* was more tolerant to experimental conditions than the two native species, and an unavoidable suggestion is the expansion of this non-native species in relation to the native counterparts in future scenarios of increased sea-level and saltwater intrusion. Even so, environmental stresses might lead to significant decreases in total biomass and live aboveground biomass of all three species, which would potentially weaken their ability to trap sediments and accumulate organic matter. However, the relatively high belowground-to-aboveground biomass ratio indicated phenotypic plasticity in response to stressful environmental conditions, which suggest that marsh species can adapt to sea-level rise and maintain marsh elevation.

Keywords Salt marsh · Macrophytes · Environmental gradient · Salinity · Biomass · Global changes

Handling editor: André Padial

L. Xue · X. Li (✉) · Z. Yan · Q. Zhang ·
W. Ding · X. Huang · B. Tian · Z. Ge
State Key Laboratory of Estuarine and Coastal Research,
East China Normal University, Shanghai 200062, China
e-mail: xzli@sklec.ecnu.edu.cn

L. Xue
xuebs21@163.com

Z. Yan
e-mail: zzyan@sklec.ecnu.edu.cn

Q. Zhang
e-mail: kilokilo@vip.qq.com

W. Ding
e-mail: dingwenhui2009@163.com

X. Huang
e-mail: hx_wxp@163.com

B. Tian
e-mail: btian@sklec.ecnu.edu.cn

Z. Ge
e-mail: zmge@sklec.ecnu.edu.cn

Q. Yin
Shanghai Chongming Dongtan Wetland Park,
Shanghai 202162, China
e-mail: yqx_michael@126.com

Introduction

Estuarine wetlands are some of the most valuable ecosystems in the world, providing a wide range of ecological functions and ecosystem services to humans including climate regulation, water purification, coastal protection, and maintenance of endangered species' habitat (Barbier et al., 2011; Luisetti et al., 2014; Ma et al., 2014). As the key component of estuarine ecosystems, halophytes are remarkable plants that complete their life cycles in environments in which the salt concentration is around 200 mM NaCl (salinity 12 ppt) or more (Flowers & Colmer, 2008). These plants have a tremendous capacity to capture carbon dioxide (CO_2) from the atmosphere through photosynthesis, then store the organic compounds in plant tissues and soils (Sousa et al., 2010a; Mcleod et al., 2011). Halophytes also play a crucial role in maintaining marsh surface elevation to keep pace with rising sea-level (Morris, 2007; Mudd et al., 2010; Baustian et al., 2012; Mueller et al., 2016). Therefore, studies evaluating how environmental changes affect halophyte performances are key to predict changes in estuarine ecosystem functioning.

Estuarine wetlands have recently been identified as important natural carbon sinks (Hopkinson et al., 2012; Artigas et al., 2015; Mueller et al., 2016), which is partly attributed to their extremely high primary productivity (Darby & Turner, 2008; Kathilankal et al., 2008; Sousa et al., 2010b; Mcleod et al., 2011) and high efficiency at trapping terrestrial and oceanic suspended sediments during tidal inundation (Baustian et al., 2012; Morris et al., 2013; Regnier et al., 2013; Hyndes et al., 2014), as well as the incomplete decomposition of organic matter and plant detritus under saline, anoxic conditions (Hu et al., 2014; Lewis et al., 2014). Carbon is returned to the atmosphere as CO_2 or methane (CH_4) through respiration and decomposition (Melton et al., 2012; de Klein & van der Werf, 2014). In the case of substantial sulfate ion concentrations, the inhibitory effects of SO_4^{2-} on CH_4 emissions are discernible in salt marshes (Chmura et al., 2003; Poffenbarger et al., 2011; Kang et al., 2012). Accordingly, enhanced carbon emissions caused by conversion and degradation of estuarine ecosystems should be included in marsh carbon budgets (Pendleton et al., 2012; Theuerkauf et al., 2015).

Due to the unique position at the interface between land and ocean (Gillanders et al., 2011; Jennerjahn & Mitchell, 2013; Osland et al., 2016) with riverine input, estuarine wetlands are considered ecotone/transition zone that are highly susceptible to pronounced, interactive, unpredictable, and irreversible damage from global climate change, as well as other anthropogenic activities (Gedan et al., 2009; Kirwan & Mudd, 2012; Kirwan & Megonigal, 2013). Indeed, species invasions are common threats in estuaries, and comparison of native and non-native halophyte performances to environmental changes may reveal changes in ecosystem functioning due to changes in the dominant halophyte (Diskin & Smee, 2017).

It is generally accepted that the distinctive plant zonation patterns along elevation gradients may be strongly regulated by interspecific relationships (i.e., facilitation and competition) and the physical environment, particularly soil salinity and tidal inundation (Engels et al., 2011; Brownstein et al., 2013), which are directly associated with elevation of marsh surfaces relative to mean sea-level (Colmer et al., 2013; Morris et al., 2013). Halophytes inhabit and thrive under harsh environmental conditions, reflecting their high tolerance to abiotic stressors (Pennings et al., 2005; Davy et al., 2011).

However, adaptations to counteract stresses have physiological maintenance costs in halophytes, and biomass production can be taken as a proxy for characterizing the amount of energy that went into growth after accounting for maintenance costs (Spalding & Hester, 2007). In general, biomass accumulation and allocation at any given time are driven by both genes and the environment. There are common patterns (allometric relationships) to match the physiological activities and functions performed by various organs (stems, leaves, and roots) (Niklas & Enquist, 2002; Poorter et al., 2012). In some demanding environments, such situations can be greatly modified by phenotypic plasticity to improve plants' fitness (Functional equilibrium hypothesis) (Funk, 2008; Pfennig et al., 2010; Freschet et al., 2015). When the foundation plant species in estuarine wetlands are perturbed by a series of abiotic stressors that affect their aboveground and/or belowground growth or alter species composition, large effects on ecosystem stability and carbon storage may result (Kirwan & Megonigal, 2013; Osland et al., 2016).

As common environmental stressors, salinity and inundation often co-vary with elevation within the tide range under field conditions. In this study, we conducted controlled experiments to subdivide the above stressors into three aspects (flooding salinity, flooding depth, and flooding frequency) to quantitatively analyze their independent impacts on two native dominant halophytes (*Phragmites australis*, and *Scirpus mariqueter*) and on the non-native and invasive *Spartina alterniflora* in the Yangtze River Estuary, China. Our specific objectives were: (1) to investigate the responses of biomass accumulation and allocation to the gradients of flooding salinity, flooding depth, and flooding frequency among species; and (2) to quantify the relationships between these environmental variables and biomass accumulation of halophytes. We hypothesized that the controlled environmental stresses would exert significant negative effects on biomass of the three halophytes, but effects may depend on the origin of halophyte (native vs. non-native).

Materials and methods

Site description

Controlled outdoor pot experiments were conducted during the growing season (April–October) in 2014 in the open space near the Dongtan Wetland Park (31°31′N, 121°56′E). All experimental treatments were exposed to ambient temperature and humidity without any roof. The seedlings and soil for experiments were collected from the salt marsh in the Chongming Dongtan Nature Reserve (31°25′–31°38′N, 121°50′–122°05′E), which is located at the eastern part of the Yangtze River Estuary, China. Before the intentional introduction of *S. alterniflora* (an exotic C4 grass native to North America) for erosion control, soil amelioration, and dike protection in the 1990s, the Dongtan salt marsh was mainly dominated by two native species: *P. australis* and *S. mariqueter* (Li et al., 2009, 2014). Due to rapid expansion through both asexual and sexual reproduction, the area occupied by *S. alterniflora* increased to 80.4 km^2, accounting for 39% of the total vegetated salt marsh of the Yangtze River Estuary in 2010 (Li et al., 2014). Thereafter, the typical plant zonation patterns along elevation gradients appeared as "mudflat—*S. mariqueter*—*P. australis*" and "mudflat—*S. mariqueter*—*S. alterniflora*—*P. australis*" (He et al., 2011; Tang et al., 2014). Recently, a project to control *S. alterniflora* and promote reestablishment of the *S. mariqueter* community was launched by the local government, which has significantly altered the vegetation distribution patterns. As a result, the continuous expansion of *S. alterniflora* has apparently slowed.

The Yangtze River Estuary has an eastern Asian monsoon climate with an average annual temperature ranging from 15.2 to 15.8°C, an average annual precipitation of 1022 mm, and an average humidity of 82%. The Dongtan salt marsh is characterized by an irregular semi-diurnal tide with maximum and mean tide ranges of 4.62–5.95 and 1.96–3.08 m, respectively (Ge et al., 2016). According to a report from the Chinese State Oceanic Administration (SOA) in (2016), sea-level rise in the coastal area has occurred at a rate of 3.7 mm year^{-1} in the last several decades (1993–2015), which is higher than the mean rate of global sea-level rise of 3.2 mm year^{-1} between 1993 and 2010 (IPCC, 2013). Due to construction of the Three Gorges Dam and implementation of the South-to-North Water Transfer Project, runoff and sediment input to the Yangtze River Estuary have decreased dramatically, which could further exacerbate the impacts of sea-level rise and result in saltwater intrusion, coastal erosion and other problems. For example, saltwater intrusion was sustained for more than 23 days in February 2014, which was higher than previous records for the period (SOA, 2015).

Experimental design

To establish controlled treatments to simulate the potential impacts of sea-level rise and saltwater intrusion, it was necessary to identify soil salinity and flooding regimes that halophytes were subjected to in the natural salt marsh. Soil salinity gradually increases with elevation gradients from low marsh to high marsh, reaching the maximum at the intertidal zone above the mean high water level because of the combined effects of infrequent submergence and intensive evapotranspiration (Silvestri et al., 2005; He et al., 2009). Flooding salinity was generally considered one of the most important factors regulating the spatial pattern of soil salinity, which was ultimately determined by the ratio between seawater and freshwater. In our study area, flooding salinity varied greatly at different temporal and spatial scales, and the salinity of soil pore water typically ranged from 4 to 18 ppt (Tang et al., 2014). As a result, we mainly focused on the flooding salinity experiments without considering other factors, such as precipitation, evapotranspiration, and biological absorption/excretion, which had heterogeneous characteristics that made their contributions to soil salinity variation difficult to quantify. The experimental flooding salinity treatments applied consisted of six levels ranging from freshwater to seawater (0, 5, 10, 15, 25, and 35 ppt).

Flooding regimes generally contain three main components: magnitude, frequency, and duration (Steinman et al., 2014). Duration was precluded from this study because both tide cycles in a day usually sustained about 4–6 h from flood to ebb tide (based on the tide tables in 2014 at Nanbao Station, Yangtze River Estuary, China). There was no distinct difference in flooding duration between low marsh and high marsh during a flood-ebb cycle. Regarding the magnitude, *P. australis*, *S. alterniflora*, and *S. mariqueter* inhabited the Dongtan salt marsh with typical plant zonation patterns from high marsh to low marsh. Without regard to storm surges and other extreme weather events, the flooding depths that these species experienced were mainly influenced by the tide, which could be obtained indirectly by subtracting the elevations that these species inhabited from the heights of the tide that they experienced. The mean elevations of the *P. australis* zone (Mean ± SD: 3.75 ± 0.57 m, $n = 1248$), *S. alterniflora* zone (Mean ± SD: 3.55 ± 0.73 m, $n = 404$), and *S. mariqueter* zone (Mean ± SD: 3.25 ± 0.72 m, $n = 331$) were referenced from Ding et al. (2015). Tide heights were recorded every hour at Nanbao Station in 2014. After analyzing the variations of flooding depth over an entire year (8760 h), we found that the probabilities of flooding depths at the range of 0–80 cm were close to 99.8, 99.5, and 97.6% for the *P. australis* zone, *S. alterniflora* zone, and *S. mariqueter* zone, respectively. Their inundation was mainly concentrated (over 85%) at depths less than 50, 60, and 72 cm, respectively. Consequently, six flooding depth levels (0, 10, 20, 40, 60, and 80 cm) were established to quantify their potential impacts. Some water (flooded until reaching the maximum soil moisture content, approximately 200 ml per pot) was provided for halophytes at 0 cm to prevent drying during drought.

Regarding the frequency, tide ranges were widely known to be varied semi-monthly, and there was one spring tide and one neap tide in a 15-day cycle. Variations in marsh elevation resulted in a gradient in flooding frequency, where the high elevations were inundated once every 15 days during the spring tide, the low elevations were inundated everyday, and the intermediate elevations captured the full range of tidal inundation from every 15 days to daily. The present study was conducted to explore the effects of tidal inundation on halophytes in the intertidal zone of the Dongtan salt marsh. The supratidal zone that never flooded under regular conditions was beyond the range of this study. Therefore, five flooding frequency levels (every day, every 3 days, every 7 days, every 10 days, and every 15 days) were deployed to analyze the probable influences on halophytes. Levels of treatment factors (flooding salinity, flooding depth, and flooding frequency) were manipulated independently, and the two factors not of interest in a particular set of trials were maintained at their least-stressful level across all levels of the manipulated factor. Interactions between treatment factors were therefore not examined in this study (See Fig. 1 for more details). Additionally, the irregular semi-diurnal tide cycle was simplified and conducted regularly twice a day, from 5 am to 9 am, and from 5 pm to 9 pm.

Implementation methods

Seedlings of *P. australis*, *S. alterniflora*, and *S. mariqueter* and soil (up to 30 cm depth, undisturbed and homogeneous) were excavated from the intertidal zone of Dongtan salt marsh and transported immediately to plastic pots (height = 30 cm, $\text{diameter}_{\text{top}} = 32$ cm, $\text{diameter}_{\text{bottom}} = 26$ cm) in early April of 2014. For each species, specimens were selected at random from a monospecific population with similar phenotypes to minimize differences in height, density, health status, and even genotypes. After being transplanted, seedlings of *P. australis* and *S. alterniflora* were trimmed at the soil surface. The plant height of *S. mariqueter* was shorter than 5 cm and thus not trimmed. The number of stems per pot in *P. australis*, *S. alterniflora*, and *S. mariqueter* was about 48 ± 9 (Mean ± SD, $n = 51$), 12 ± 2 (Mean ± SD, $n = 51$), and 306 ± 32 (Mean ± SD,

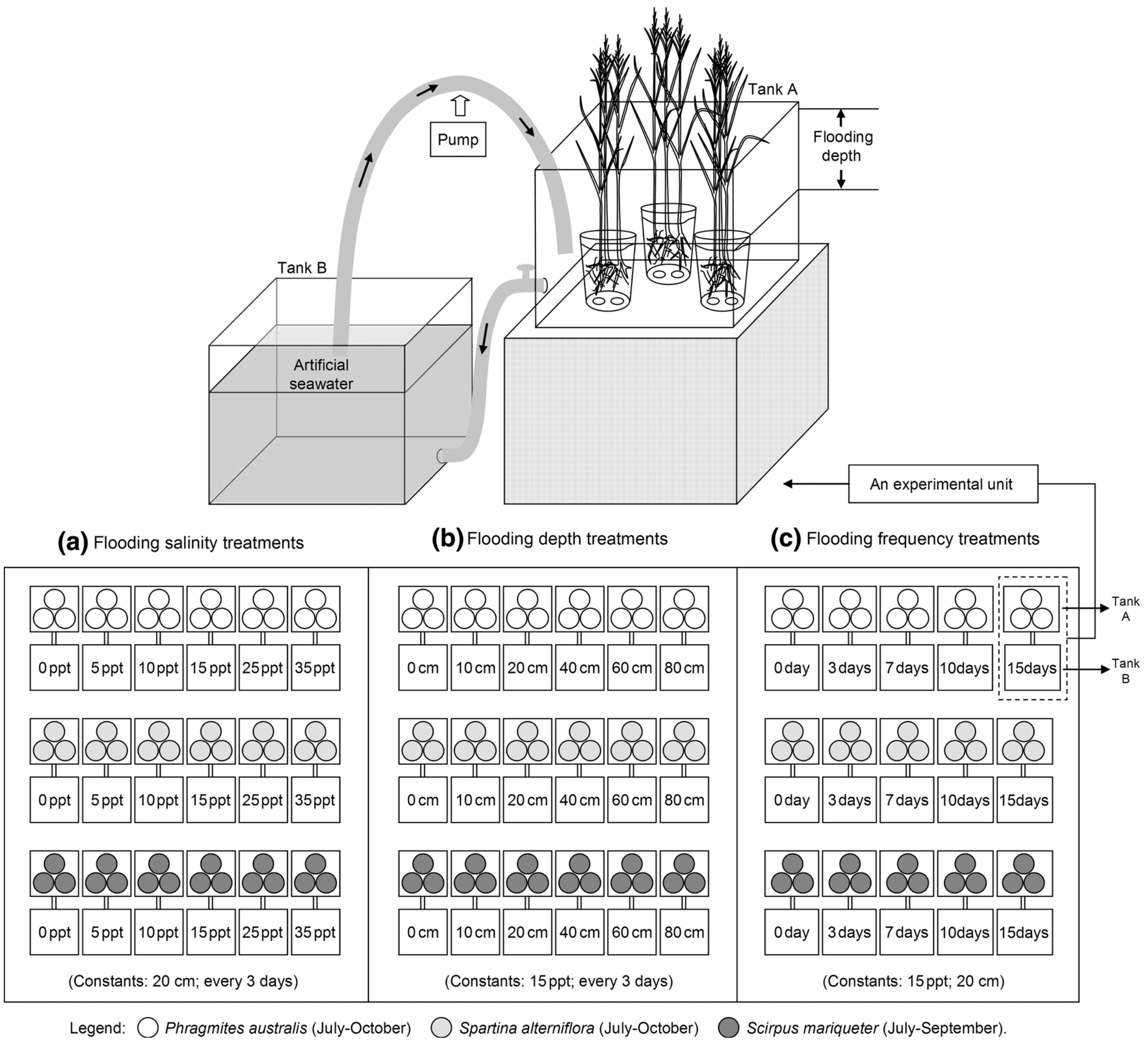

Fig. 1 Schematic representation of the experimental design. *Note* Each treatment was conducted twice a day (from 5 am to 9 am, and from 5 pm to 9 pm) to simulate two tide cycles in one day

$n = 51$), respectively. All pots were maintained under common garden conditions until the beginning of the controlled experiments, and they were watered every 2 days (about 200 ml each time) with coarsely filtered canal water with a salinity that generally ranged from 2 to 5 ppt. The treatments for *P. australis* and *S. alterniflora* were conducted from July to October for about 4 months, while the treatments for *S. mariqueter* ran for about 3 months from July to September because of the early senescence of this species.

An experimental unit was composed of two transparent plastic tanks (width = 76 cm, length = 97 cm, height = 70 cm), one with three pots of the same species as three replicates, and the other with salt water (Fig. 1). Two tanks were connected to each other through a tube (length = 100 cm, diameter = 25 mm) and controlled by taps. To mimic the situation in the field in which halophytes could absorb moisture from the deep soil, regardless of whether they were inundated or exposed to the atmosphere, approximately 5 cm of water (Fig. 1 tank A) was kept during the non-flooded period to protect halophytes from drought and death in summer. All pots were perforated with two 3-cm-diameter holes for vertical water exchange. For the 0 cm level in flooding depth treatments for all three species, no water was maintained in the tanks. Larger transparent plastic buckets (height = 135 cm, diameter = 100 cm) were used for the relatively high flooding depth levels (40, 60, and 80 cm). A rising tide was simulated by pumping in salt water (pumps: caliber 25 mm, watt 750, flow velocity 60 l/min). At the end of a treatment cycle, salt water was pumped out or allowed to flow back by gravity because the two tanks in a unit were anchored at different heights. Several pumps worked together to ensure all treatments were conducted within 45 min, which were not included in the flooding time (about 4 h).

The flooding salinity levels for controlled treatments were obtained by mixing commercially available sea salt (Shenzhen Jinchuangxing Industrial Co. Ltd, China) with water from a nearby canal. The canal water was cleaned through subsiding and filtration to prevent algae in the tanks; however, no algaecide was used. Before implementing the experimental treatments, the salt concentration of each tank was monitored using an automatic compensation salinity refractometer (Master-S/Millα, Cat. No. 2491, ATAGO, Japan) and corrected to the initial conditions, either by adding water or sea salt. The saline and hypersaline water were recirculated and renewed every 2 weeks, whereas the freshwater collected from the clean tap water and rainwater was only passed through the tidal pumping system once. Pots were rotated regularly to minimize the possible impacts of position, and weeded every 2 weeks to avoid nutrient competition from unintended species. Damage from insects and pathogens was not detected throughout the controlled experiments.

Measurements and analyses

At the end of controlled experiments, the aboveground biomass (AGB) for *P. australis* and *S. alterniflora* was clipped at the soil surface from each pot in early November 2014, while *S. mariqueter* was harvested 1 month earlier in October 2014. All individuals of the same species were harvested on the same day, and separated into different fractions (stem, leaf, seed, and litter). It should be noted that the leaf sheath of *S. mariqueter* was incorporated into the leaf portion, with no stem material designated for this species. With the exception of litter, the aforementioned fractions were summed to obtain live AGB, while litter was considered dead AGB. These separated plant samples were sealed in pre-labeled paper bags and subsequently transported to the laboratory in Dongtan Wetland Park. After oven drying at 60°C for approximately 72 h, we measured the dry weight (DW) to the nearest 0.1 g. Belowground biomass (BGB) was obtained using cores constructed of polyvinyl chloride pipes (length = 100 cm, diameter = 7 cm) with sharpened edges. Three 30-cm-long sediment cores were randomly collected from each pot after the AGB was removed. Each core was extruded and washed in a mesh bag with 0.15 mm sieve to prevent the loss of fine and dead root materials. The roots and rhizomes were combined to obtain the BGB after drying at 60°C to constant weight. Total biomass (TB) was calculated as the sum of all portions collected (stem, leaf, seed, litter, and root system), or the sum of the total AGB (live and dead) and BGB. Biomass in different parts or in whole plants was estimated as g m^{-2} of dry mass, and the BGB represented the dry root materials in top soil (0–30 cm). We also randomly collected soil samples from the top soil (0–10 cm) with a stainless steel cylinder (height = 5 cm, diameter = 5 cm) in each pot every month to characterize the soil conditions. Soil electric conductivity was measured using a digital conductivity meter (DDS-11A, 10^4 μS/cm, Shanghai REX Instrument Factory, China), then converted into soil salt content of dry soil (g kg^{-1}).

All data analyses were conducted using SPSS (IBM Corporation, version 22.0), and figure plots were generated using OriginPro (OriginLab Corporation, version 9.0). Data were tested for normality and homogeneity of variance using the Kolmogorov–Smirnov test and Levene's test. Logarithm, arcsine, and square-root transformation were conducted to meet the assumptions for statistical analyses. One-way analysis of variance was used to test the statistical significance of environmental variables on the biomass accumulation and allocation. When significant differences were detected (significance level at $P <$ 0.05 in all cases), subsequent multiple comparison (the least significant difference test, LSD test) was applied to determine differences among treatments. Regression analyses were implemented to evaluate rates of change in biomass accumulation across the environmental gradients.

Results

Biomass accumulation

As expected, there were significant decreases in stem biomass ($F_{5,12} = 13.96$, $P < 0.001$), leaf biomass ($F_{5,12} = 59.04$, $P < 0.001$), and seed biomass ($F_{5,12} = 17.40$, $P < 0.001$) for *P. australis* subjected to increasing flooding salinity (Fig. 2a–c). The sexual reproduction capacity (seed biomass) of *P. australis* was completely inhibited at high levels of flooding salinity stress (25 and 35 ppt), with the corresponding soil salinity up to 5.5–6.5 g kg^{-1}. Stem ($F_{5,12} = 21.92$, $P < 0.001$), leaf ($F_{5,12} = 15.50$, $P < 0.001$), and seed ($F_{5,12} = 5.31$, $P = 0.008$) biomass of *S. alterniflora* was also significantly decreased in response to high levels of flooding salinity (Fig. 2a–c), while litter biomass of *S. alterniflora* showed no significant difference among the flooding salinity levels (Fig. 2d). *S. mariqueter* was more sensitive than the other two species to gradual changes in flooding salinity, resulting in a greater decrease (100%) in leaf biomass ($F_{5,12} = 67.46$, $P < 0.001$) than for *P. australis* (81.8%) and *S. alterniflora* (73.7%) at high salt concentration (35 ppt) when compared to the responses in freshwater (0 ppt) (Fig. 2b). The decrease in seed biomass ($F_{5,12} = 33.26$, $P < 0.001$) for *S. mariqueter* (81.9%) was higher than for *S. alterniflora* (39.1%) from freshwater (0 ppt) to seawater (35 ppt) (Fig. 2c). No significant differences were observed in the BGB (root + rhizome) for the three species within any of the six flooding salinity levels ($P > 0.05$) (Fig. 2e). TB for all three species also substantially decreased because of significant decreases in their live aboveground parts, indicating that the trends in TB were not counterbalanced by insignificant BGB changes (Fig. 2f).

Elevated flooding depth also significantly decreased the stem biomass ($F_{5,12} = 3.21$, $P = 0.046$), seed biomass ($F_{5,12} = 14.78$, $P < 0.001$), and litter biomass ($F_{5,12} = 5.40$, $P = 0.008$) of *P. australis* (Fig. 3a, c, d), as well as the leaf biomass ($F_{5,12} = 28.68$, $P < 0.001$) and seed biomass ($F_{5,12} = 24.42$, $P < 0.001$) of *S. mariqueter* (Fig. 3b, c). However, BGB of *P. australis* and *S. mariqueter* were not significantly affected by flooding depth ($P > 0.05$) (Fig. 3e). In contrast, there were no clear tendencies in the biomass of different parts of *S. alterniflora* among the flooding depth treatments, with relatively low stem biomass and litter biomass being observed at 0 cm (Fig. 3a, d).

Before implementing the flooding depth treatments, there was no significant difference in soil salinity within the same species for *P. australis* (Mean ± SD: 1.6 ± 0.2 g kg^{-1}, $n = 18$), *S. alterniflora* (Mean ± SD: 2.2 ± 0.3 g kg^{-1}, $n = 18$), and *S. mariqueter* (Mean ± SD: 2.4 ± 0.3 g kg^{-1}, $n = 18$). As the flooding depth treatments were processed, we found that the 0 cm level had few negative effects on the accumulation of soil salinity because of the limited input of salt. No significant differences in soil salinity were observed among the rest of the flooding depth levels (10–80 cm) within the same species during each month ($P > 0.05$). In this regard, the performance of halophytes in flooding depth treatments (10–80 cm) was mainly dependent on the flooding depth levels and not soil salinity. Elevated flooding depths from 10 cm to 80 cm for about 3–4 months in this flooding depth experiment did not significantly influence the TB accumulation for *P. australis* and *S. mariqueter* (Fig. 3f). Moreover, covering by medium saline water (15 ppt) at various flooding depths (10–80 cm) led to increases in the TB of *S. alterniflora* when compared to the relatively dry environment (0 cm) (Fig. 3f).

As the most sensitive organ of halophytes, the biomass accumulation of seeds for *P. australis* and *S. mariqueter* increased significantly with decreasing flooding frequency from every day to every 15 days (Fig. 4c). When considered with stem and leaf biomass, the live AGB for all three species was not statistically significant ($P > 0.05$). Moreover, there were no significant differences in BGB and TB among different flooding frequency levels ($P > 0.05$) for *P. australis*, *S. alterniflora*, and *S. mariqueter* (Fig. 4e, f). However, it is important to note that soil salinity may be partly responsible for the inhibitory effects of frequent flooding treatments on biomass accumulation of halophytes based on the monthly changes of soil salinity in the flooding frequency experiment.

Regression analyses were conducted to describe the direction and extent of the significant responses for each species. Biomass in different live aboveground parts (stem, leaf, and seed) of these species all decreased significantly with increasing soil salinity. About 50.5, 48.6, and 76.8%, and 74.7, 70.6, and 34.5% of the biomass variations in stems, leaves, and seeds from *P. australis* (Fig. 5a–c) and *S. alterniflora* (Fig. 5f–h) were caused by gradient changes in soil salinity. Similarly, soil salinity could explain 69.7 and 67.8% of the variations in leaf biomass and seed

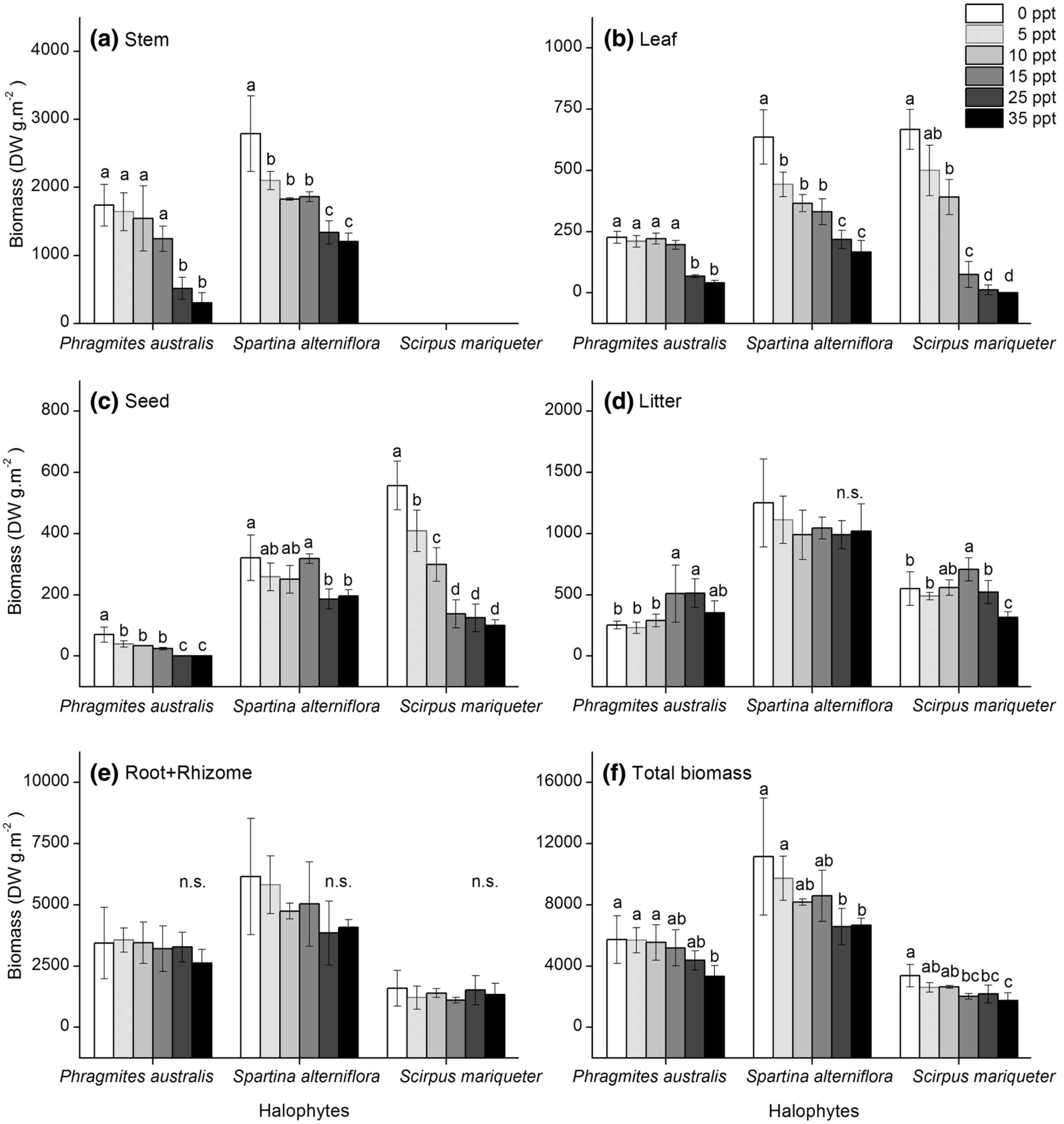

Fig. 2 Variations in biomass (Mean ± SD, $n = 3$) of three dominant halophytes in the Yangtze River Estuary following exposure to six flooding salinity levels (0, 5, 10, 15, 25, and 35 ppt) after a growing season, while the flooding depth (20 cm) and flooding frequency (every 3 days) were constant. *Note* Different small letters indicate significant differences ($P < 0.05$) among treatments of the same group according to the LSD test; "n.s." indicates no significant difference among treatments

biomass for *S. mariqueter*, respectively (Fig. 5k, l). The contribution of soil salinity to variations in live AGB (Fig. 5d, i, m) and TB (Fig. 5e, j, n) for *P. australis*, *S. alterniflora*, and *S. mariqueter* was about 52.2, 73.2, and 70.0%, and 26.1, 38.2, and 44.0%, respectively.

The 0 cm treatments were precluded from regression analyses between flooding depth and biomass accumulation of the three halophytes because their corresponding soil salinity was significant lower than those of other flooding depth treatments (10–80 cm) ($P < 0.05$). Only *P. australis* and *S. mariqueter*

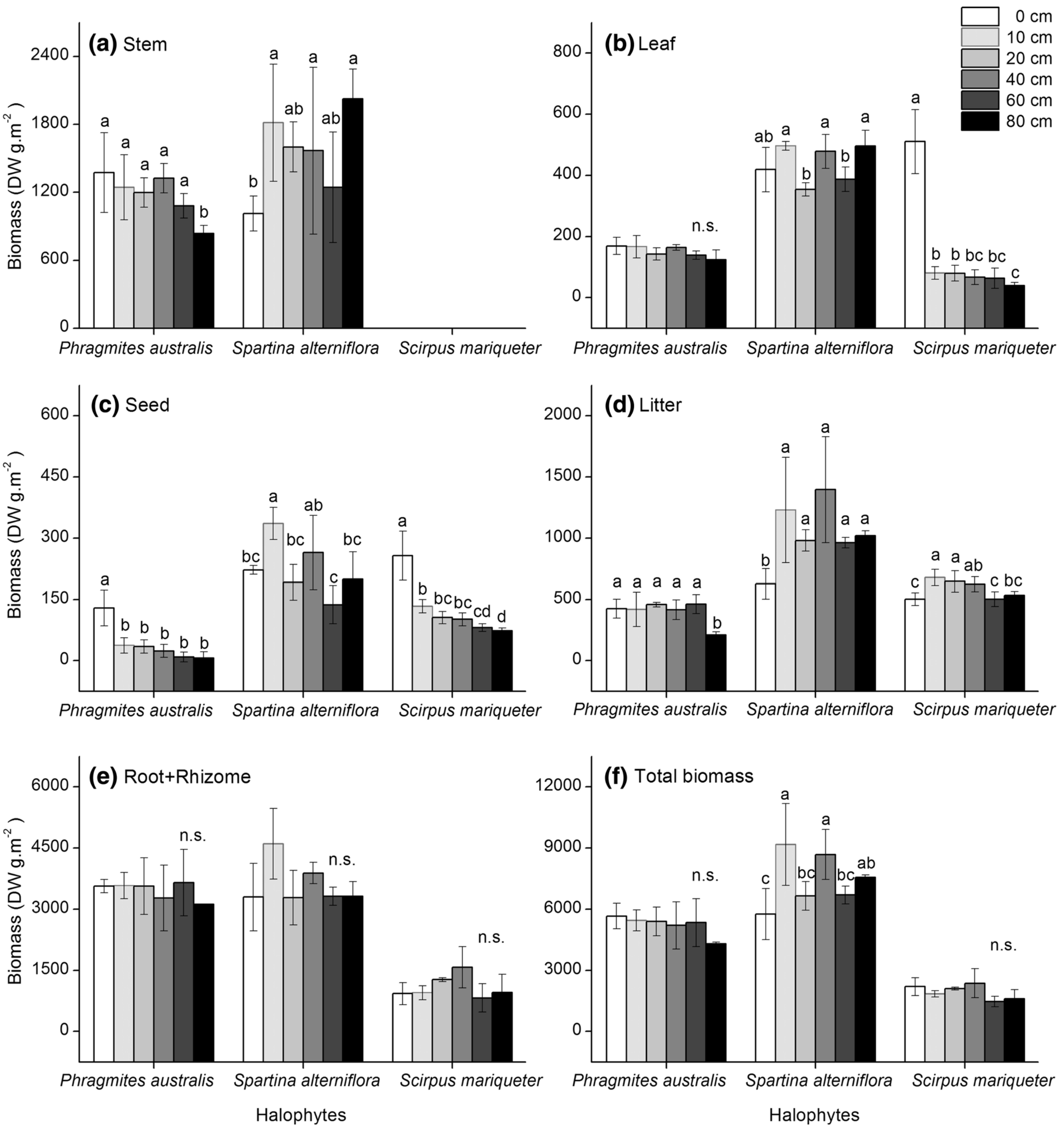

Fig. 3 Variations in biomass (Mean ± SD, $n = 3$) of three dominant halophytes in the Yangtze River Estuary following exposure to six flooding depth levels (0, 10, 20, 40, 60, and 80 cm) after a growing season, while the flooding salinity (15 ppt) and flooding frequency (every 3 days) were constant. Some water (flooded until reaching the maximum soil moisture content, approximately 200 ml per pot) was provided at the 0 cm level. *Note* Different small letters indicate significant differences ($P < 0.05$) among treatments of the same group according to the LSD test; "n.s." indicates no significant difference among treatments

responded significantly to changes in flooding depth (10–80 cm). About 65.2 and 63.7% of the biomass variations in stems and seeds for *P. australis* (Fig. 6a, b), as well as 31.5% and 71.9% of the biomass variations in leaves and seeds for *S. mariqueter* (Fig. 6g, h), were attributed to the increase of flooding depths. The relationship between live AGB of *P. australis* and flooding depth (10–80 cm) was hump-

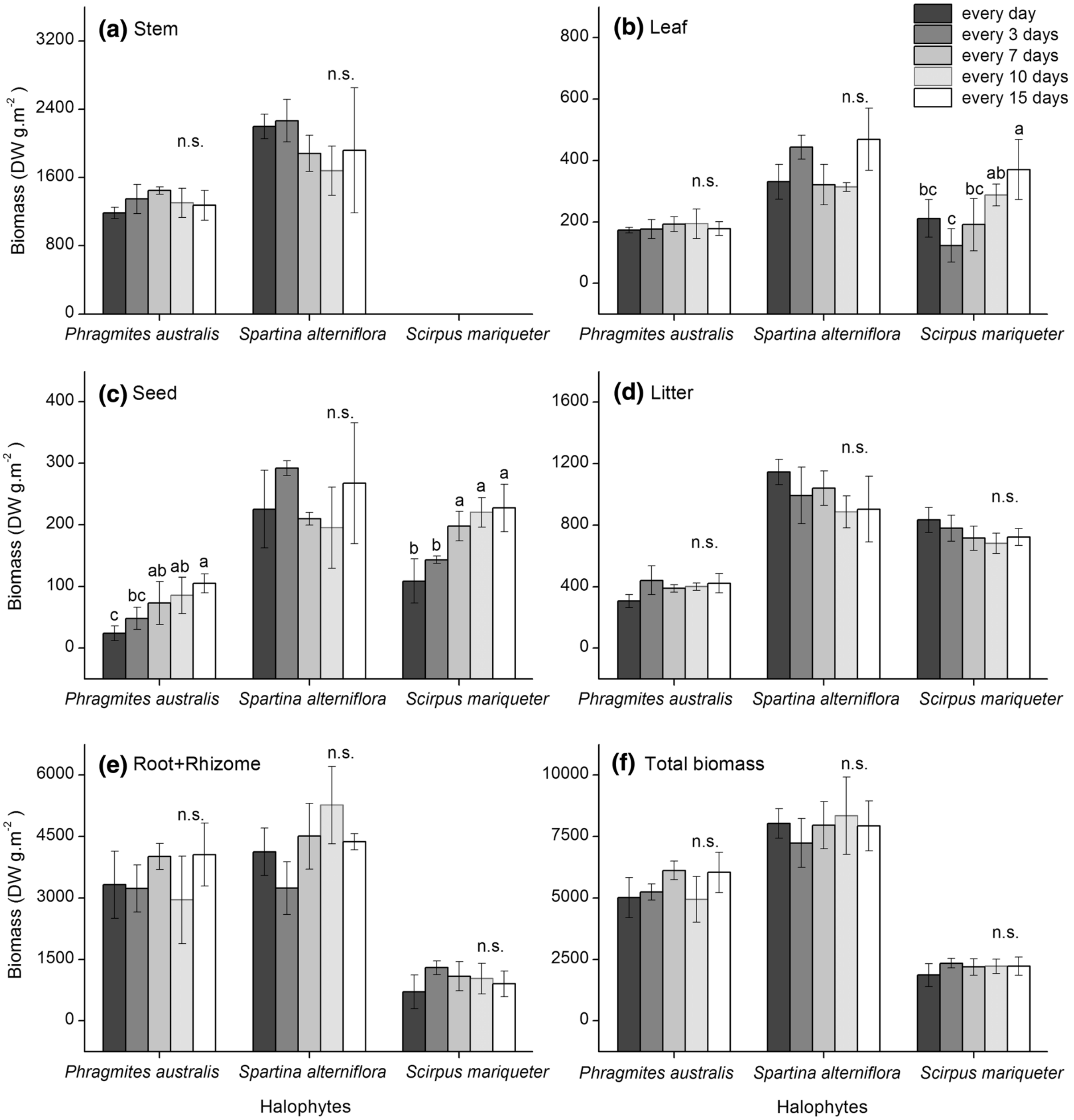

Fig. 4 Variations in biomass (Mean ± SD, $n = 3$) of three dominant halophytes in the Yangtze River Estuary following exposure to five flooding frequency levels (every day, every 3 days, every 7 days, every 10 days, and every 15 days) after a growing season, while the flooding salinity (15 ppt) and flooding depth (20 cm) were constant. *Note* Different small letters indicate significant differences ($P < 0.05$) among treatments of the same group according to the LSD test; "n.s." indicates no significant difference among treatments

shaped, with the value first rising and then decreasing with increased depth and peaking at a flooding depth of 40 cm above the soil surface (Fig. 6c). In contrast, the live AGB of *S. mariqueter* declined directly with increasing flooding depth (Fig. 6i). Based on the coefficients of determination in regression equations, the flooding depth (10–80 cm) treatments could explain 65.2 and 65.9% of the variations in the live AGB for *P. australis* and *S. mariqueter*, respectively.

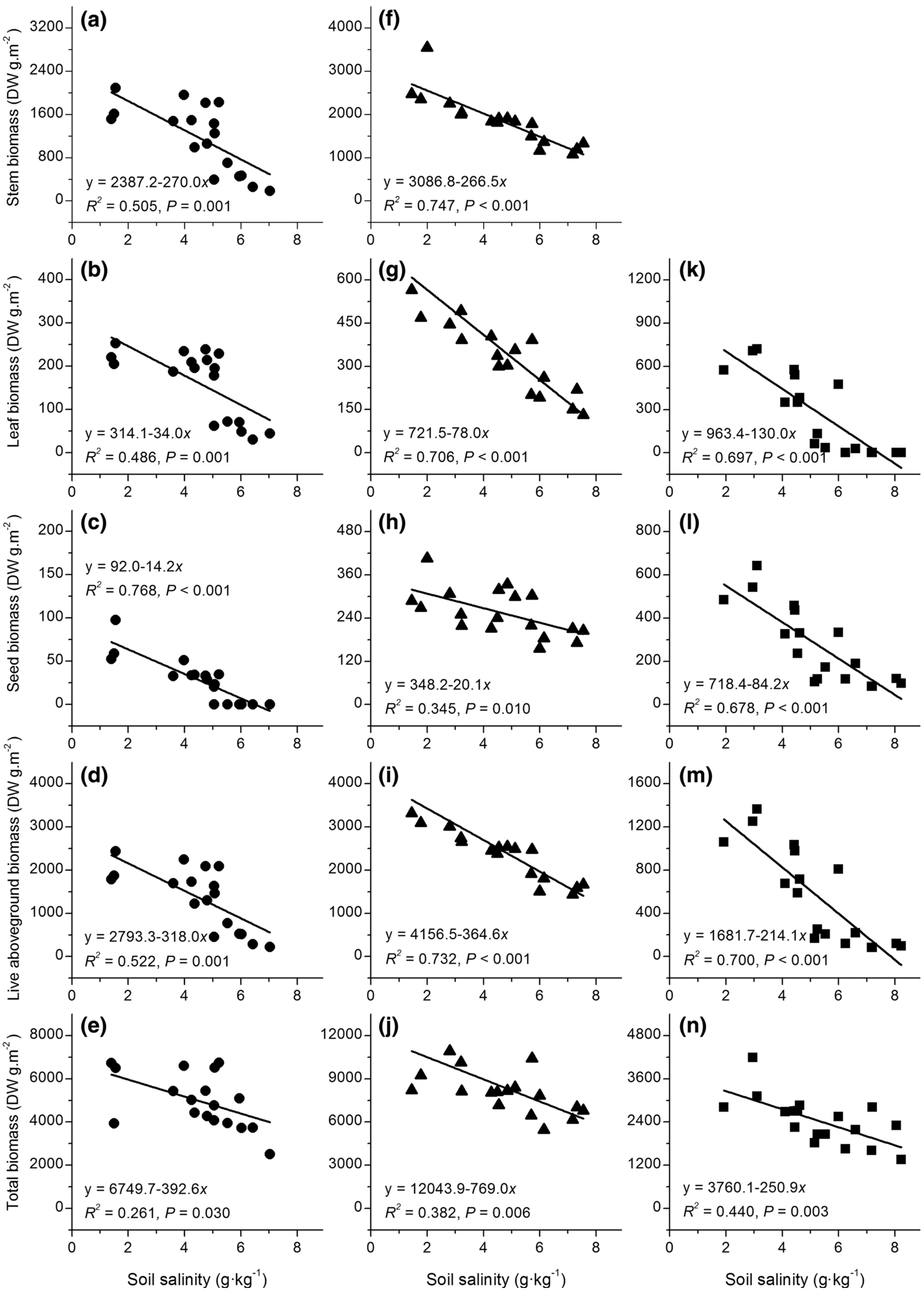
(a)
Stem biomass (DW g.m^{-2})
y = 2387.2-270.0x
R^2 = 0.505, P = 0.001
(f)
y = 3086.8-266.5x
R^2 = 0.747, P < 0.001
(b)
Leaf biomass (DW g.m^{-2})
y = 314.1-34.0x
R^2 = 0.486, P = 0.001
(g)
y = 721.5-78.0x
R^2 = 0.706, P < 0.001
(k)
y = 963.4-130.0x
R^2 = 0.697, P < 0.001
(c)
Seed biomass (DW g.m^{-2})
y = 92.0-14.2x
R^2 = 0.768, P < 0.001
(h)
y = 348.2-20.1x
R^2 = 0.345, P = 0.010
(l)
y = 718.4-84.2x
R^2 = 0.678, P < 0.001
(d)
Live aboveground biomass (DW g.m^{-2})
y = 2793.3-318.0x
R^2 = 0.522, P = 0.001
(i)
y = 4156.5-364.6x
R^2 = 0.732, P < 0.001
(m)
y = 1681.7-214.1x
R^2 = 0.700, P < 0.001
(e)
Total biomass (DW g.m^{-2})
y = 6749.7-392.6x
R^2 = 0.261, P = 0.030
(j)
y = 12043.9-769.0x
R^2 = 0.382, P = 0.006
(n)
y = 3760.1-250.9x
R^2 = 0.440, P = 0.003
Soil salinity (g·kg^{-1})
Soil salinity (g·kg^{-1})
Soil salinity (g·kg^{-1})

◀**Fig. 5** Regression relationships between soil salinity and stem biomass, leaf biomass, seed biomass, live aboveground biomass, and total biomass for *Phragmites australis* (**a**–**e**), *Spartina alterniflora* (**f**–**j**), and *Scirpus mariqueter* (**k**–**n**)

Biomass allocation

We quantified AGB and BGB allocation in the three study species and analyzed the potential influences of environmental factors. The flooding salinity treatments showed that the belowground-to-aboveground biomass ratios (BGB:AGB) for *P. australis* ($F_{5,12}$ = 14.76, $P < 0.001$) and *S. mariqueter* ($F_{5,12}$ = 7.166, P = 0.003) were significantly increased by the increasing flooding salinity (Fig. 7a). The BGB:AGB ratios for *P. australis* and *S. mariqueter* in the seawater treatments (35 ppt) reached 3.8 ± 0.2 (Mean ± SD, $n = 3$) and 3.2 ± 0.8 (Mean ± SD, $n = 3$), which were 2.5-fold and 3.6-fold of those under the freshwater treatments (0 ppt), respectively. In contrast, the response of the BGB:AGB ratio of *S. alterniflora* to gradual changes in flooding salinity levels were not significant ($P > 0.05$). In the flooding depth and flooding frequency

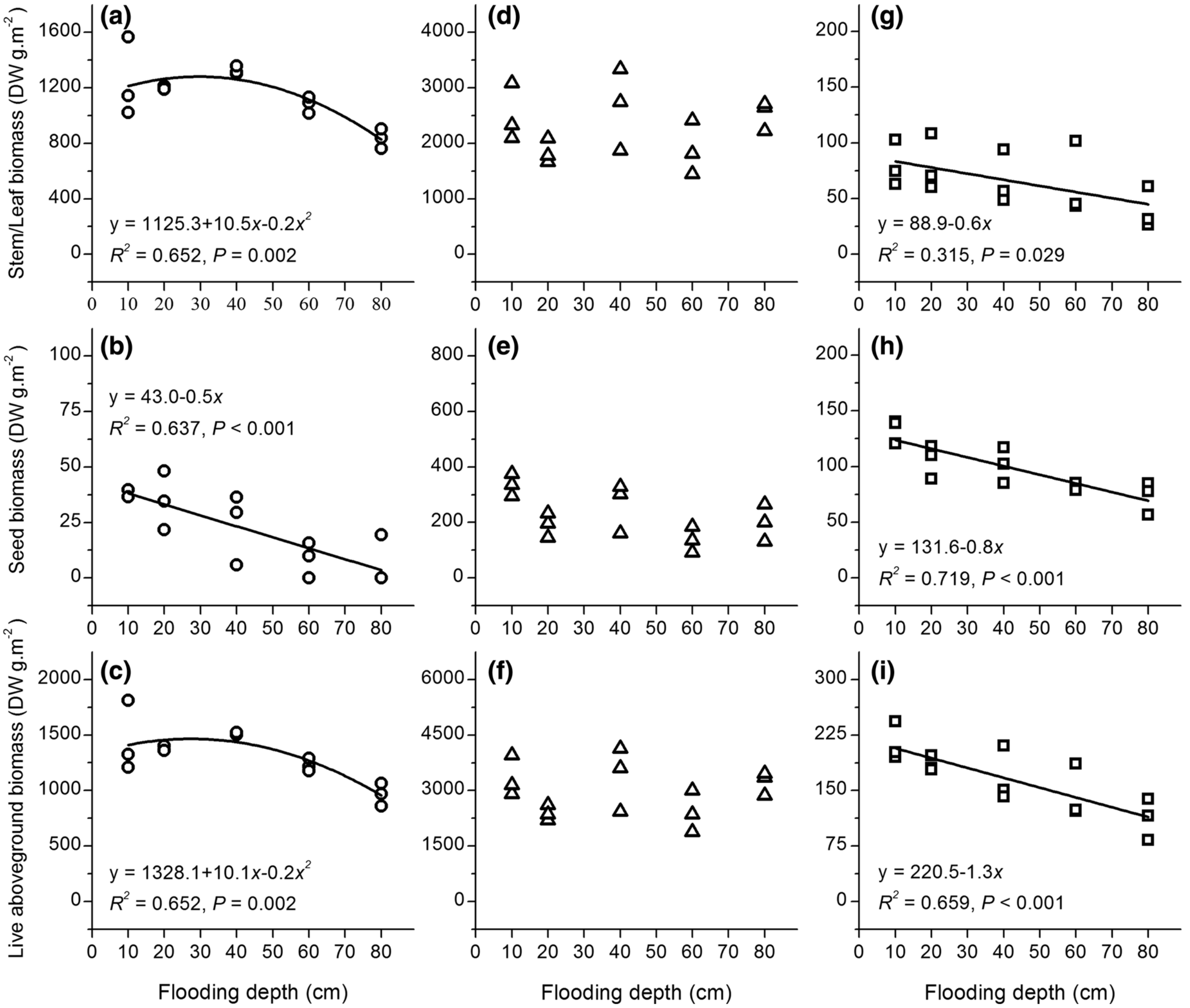

Fig. 6 Regression relationships between flooding depth (10–80 cm) and biomass accumulation of three dominant halophytes. **a**–**c** *Phragmites australis*, significant negative relationships were detected between stem biomass, seed biomass, live aboveground biomass and flooding depth (*solid lines*); **d**–**f** *Spartina alterniflora*, besides stem biomass, seed biomass, and live aboveground biomass, the remaining parts and total biomass showed insignificant relationships with flooding depth either ($P > 0.05$) (*no lines*); **g**–**i** *Scirpus mariqueter*, leaf biomass, seed biomass, and live aboveground biomass showed significant negative relationships with flooding depth (*solid lines*)

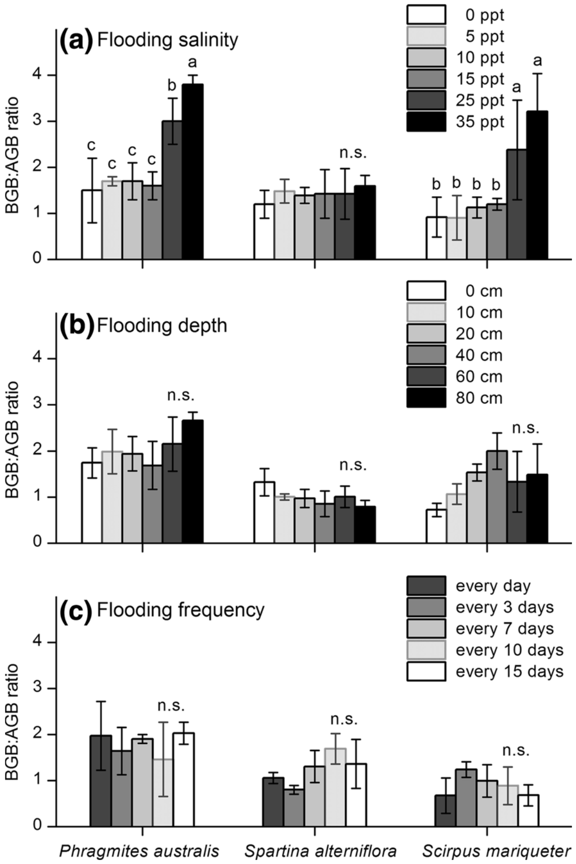

Fig. 7 Variations in biomass allocation (BGB:AGB ratio, Mean ± SD, $n = 3$) of three dominant halophytes in the Yangtze River Estuary after a growing season. **a** Flooding salinity treatments; **b** flooding depth treatments; and **c** flooding frequency treatments. *Note* Different small letters indicate significant differences ($P < 0.05$) among treatments of the same group according to the LSD test; "n.s." indicates no significant difference among treatments

treatments, there were no significant variations in the BGB:AGB ratios across species ($P > 0.05$) (Fig. 7b, c). Flooding depths and frequencies in the period of controlled experiments did not change the biomass allocation for the three species, although some differences were observed.

Discussion

Responses of halophytes biomass accumulation to variations in salinity and inundation

Soil salinity generally poses two major threats to plant growth, rapid osmotic stress, and slow ionic stress (Munns & Tester, 2008; Galvan-Ampudia & Testerink, 2011). Halophytes have evolved functional and structural adaptations to deal with soil salinity and regulate their growth in coordination with environmental constraints, resulting in the flexibility of plant morphology, which varies widely among species (Flowers & Colmer, 2008; Canalejo et al., 2014; Julkowska & Testerink, 2015). The inhibitory effects of soil salinity on biomass accumulation in halophytes has been reported in several studies based on both field measurements and controlled experiments (e.g., Onkware, 2000; Pennings et al., 2005; Wang et al., 2010; Engels et al., 2011; Tang et al., 2014). Our findings were consistent with these studies and highlighted differences in the biomass of live aboveground parts (stem, leaf and seed), as well as in TB for *P. australis*, *S. alterniflora,* and *S. mariqueter*, which significantly decreased with increasing flooding salinity from freshwater (0 ppt) to seawater (35 ppt). Relatively precise negative linear relationships were also established to quantitatively describe the adverse impacts of soil salinity on the biomass accumulation of these species, which advances the information base for these plants.

Consistent with other studies, *S. alterniflora*, a non-native species in the Yangtze River Estuary, was observed to be more tolerant to high levels of flooding salinity stress (25 and 35 ppt) than the other two species, probably because it had secretory glands allowing salt excretion and ensuring its survival under hypersaline conditions (e.g., Chen et al., 2004; Wang et al., 2006; Medeiros et al., 2013). Notably, the extra sulfate added via the addition of sea salt in the relatively high flooding salinity levels might meet *S. alterniflora*'s sulfate requirement, promoting it to thrive while threatening the growth and development of native species (Chambers et al., 1998; Medeiros et al., 2013; Sutter et al., 2015). For *S. mariqueter*, it could lead to the death of all individuals in our controlled experiments when the flooding salt concentration increased to 25 ppt or more for 2 months, while the soil salinity was approximately 5.7–6.9 g kg^{-1}. Although seed setting in *S. mariqueter* occurred from mid-June to early July, the seed biomass included the part that had already existed before the experiment began on July 1, and the seed biomass of *S. mariqueter* still significantly decreased with increased salinity gradients. If the seed setting period for *S. mariqueter* was fully covered in this experiment, the response of seed biomass to flooding salinity would be more evident than that at present, or even completely inhibited as that in *P. australis* at relatively high flooding salinity levels (25 and 35 ppt).

Flooding typically causes soils in estuarine salt marshes to become hypoxic or anoxic owing to biological consumption of O_2 without effective ventilation (Colmer & Flowers, 2008; Brownstein et al., 2013; Colmer et al., 2013), which can affect plants' abilities to undergo normal metabolic processes and cause biomass accumulation to be further restrained (Spalding & Hester, 2007). Kathilankal et al. (2008) confirmed that tidal activity can lead to reductions in midday CO_2 assimilation when compared with the non-flooded conditions on the eastern shore of the Chesapeake Bay, USA, with an average loss of 46 ± 26% (Mean ± SE). Morris et al. (2002) demonstrated that there was an optimum marsh elevation for coastal wetland productivity, that maximum production for *S. alterniflora* in the low marsh occurred at a depth of 40–60 cm below mean high tide, and growth was likely limited by hypoxia at greater depths. Kirwan & Guntenspergen (2012) observed that the shoot biomass and root production of *Schoenoplectus americanus* and *Spartina patens* followed parabolic relationships with elevation as well. The performance of *P. australis* in our flooding depth treatments was also consistent with these previous results, showing a hump-shaped curve between the live AGB and flooding depth (10–80 cm), and peaking at a flooding depth of 40 cm above the soil surface. The quadratic effect did not exist for the other two species, contrary to the results reported by Morris et al. (2002). However, a significant negative linear effect was observed between live AGB of *S. mariqueter* and flooding depth (10–80 cm). For *S. alterniflora*, elevated flooding depth did not significantly decrease the live AGB and the TB, indicating *S. alterniflora* had a greater tolerance to soil waterlogging than *P. australis* and *S. mariqueter*, especially at the flooding depth of 80 cm. In contrast, 0 cm might be more suitable for the biomass accumulation of *P. australis* and *S. mariqueter* than other flooding depths (10–80 cm) owing to the low soil salt content. Conversely, *S. alterniflora* did not show this phenomenon, suggesting that this species is relatively intolerant of drought.

Halophytes in the low marsh were exposed to more frequent flooding events than those in the relatively high marsh, which would affect the biomass accumulation (Silvestri et al., 2005; Davy et al., 2011; Colmer et al., 2013). For example, Dausse et al. (2012) reported that the minimum AGB and BGB were observed in September in the low salt marsh when compared with the fresh tidal marsh, brackish marsh, and middle salt marsh of the Dovey Estuary, UK. Negrin et al. (2012) found that the AGB for *S. alterniflora* was higher in the high marsh than the low marsh of the Bahía Blanca Estuary, Argentina, while the BGB was similar in both sites. Snedden et al. (2015) observed that the AGB and BGB were highest for *S. alterniflora* and *S. patens* at relatively high elevations when inundation was minimal, and that they declined exponentially with decreasing elevation in the Breton Sound Estuary, USA. As a result, biomass production was often closely related to the elevation of the marsh surface relative to mean sea-level. Our original objective was to identify the independent effects of environmental stressors on biomass accumulation of halophytes, especially for the flooding frequency. However, no significant differences were detected in live AGB, dead AGB, BGB, and TB for *P. australis*, *S. alterniflora*, and *S. mariqueter* among the different flooding frequency levels, which might be ascribed to the relatively short period of experimental time.

Consistent with Shelford's law of tolerance, each organism, specifically for plants in this study, had a certain minimum, maximum, and optimum environmental factor or combination of factors that determined success (Shelford, 1931). Beyond these ranges, acclimatization would fail, mortality risk would increase, or even local extinction would occur. Salinity and inundation regimes are crucial abiotic drivers in estuarine salt marshes, and sea-level rise in response to global climate change can aggravate current conditions and threaten the sustainability of estuarine wetlands. Based on our results, we assumed that the elevated flooding salinity and flooding depth caused by sea-level rise and saltwater intrusion might lead to significant decreases in live AGB of these species, especially for *P. australis* and *S. mariqueter*. Despite no significant difference being detected in the BGB among these treatments, reductions in live AGB would potentially decrease the input of organic matter to the soils. Moreover, the relatively low live AGB might weaken the ability of stems and leaves to slow water velocities, reduce erosion and enhance mineral sediment deposition (Mudd et al., 2010; Kirwan & Megonigal, 2013), thus influencing the organic matter accumulation from both organic and inorganic materials, as well as altering the ability of estuarine salt marshes to maintain their position in the intertidal zone. In fact, most coastal wetlands developed vertically at rates that were similar to or exceeded the rate of historical sea-level rise, and halophytes constantly modified the elevation of their habitat to actively resist the deleterious effects of sea-level rise (Morris et al., 2002; Kirwan & Megonigal, 2013). The continued survival of coastal wetlands was largely dependent on the combined effects of sea-level rise and human activities, and the latter was the major factor influencing historical and contemporary coastal wetland loss, especially for the Yangtze River Estuary, China.

Responses of halophytes biomass allocation to variations in salinity and inundation

Biomass allocation at any given time is regarded as a strong driver of some basic functions, such as carbon sequestration, water absorption, nutrient acquisition, and mechanical support, which could be largely modified by plant phenotypic plasticity to variable environmental conditions (Funk, 2008; Pfennig et al., 2010; Poorter et al., 2012; Freschet et al., 2015). As one of the most frequently employed expressions, the belowground-to-aboveground biomass ratio (BGB:AGB) was used to characterize the biomass allocation patterns in our controlled experiments. The results showed that the BGB:AGB ratios for *P. australis* and *S. mariqueter* were significantly elevated with increasing flooding salinity, which is consistent with the results from Scarton et al. (2002), who concluded that periodic high salinity probably led to the relatively low AGB and high BGB of *P. australis*. Roots and rhizomes were important reservoirs in the process of energy flow and material cycle in estuarine wetland ecosystems (Darby & Turner, 2008; Sousa et al., 2010a), especially for maintaining the surface elevation of salt marshes (Baustian et al., 2012; Kirwan & Guntenspergen, 2012; Mueller et al., 2016; Osland et al., 2016).

We believed that when combined with significant decreases in TB for *P. australis*, *S. alterniflora*, and *S. mariqueter* in flooding salinity treatments, increased salinity stress would limit the regular growth of *P. australis* and *S. mariqueter*, resulting in the decreased productivity of AGB and increased investment in BGB, which were considered to be the phenotypic plasticity to the harsh environments. This is consistent with previous findings regarding adaptive stress resistance, which have shown that plants grown at low temperature, low nutrient level, and low water availability showed increased biomass allocation to roots and rhizomes, while more biomass was allocated to shoots and leaves at low irradiance and low CO_2 concentrations (Moriuchi & Winn, 2004; Poorter et al., 2012; Langley et al., 2013; Freschet et al., 2015). The non-native *S. alterniflora* did not follow this pattern in the present study. If we further enhanced the flooding salinity level or extended the period of treatments, a similar tendency would be expected. Nevertheless, it was increasingly clear that the BGB:AGB ratio took stem biomass, leaf biomass, seed biomass, and litter biomass into one compartment, without quantifying their separate responses in biomass allocation to environmental conditions. Moreover, reliable estimates of root biomass were challenging owing to the root systems extending over long distances both horizontally and vertically, and because of the subjective nature of judgments used to separate live and dead roots and rhizomes. These limitations seriously hampered an objective analysis of biomass allocation patterns; therefore, resolution of these issues will enhance future analyses.

Comparison of biomass between field measurements and controlled experiments

This paper mainly focused on controlled experiments to describe the responses in biomass to simplified environmental condition gradients. There were evident advantages and disadvantages to methodologies when compared with field measurements. Rather than various abiotic stresses in the field, such as high salinity and frequent flooding, the halophytes were cultivated under favorable conditions from the middle of April to the end of June to allow recovery and acclimation to the new environments, which were conductive to their growth. This was especially relevant for *S. mariqueter*, which formed longer leaves and higher stem density than characteristic of field conditions. However, damage to halophytes during transplanting was unavoidable, which would influence the physiological activity of roots or even lead to the death of individuals. Some large halophytes often have great demands for nutrients and water. When grown in small pots, essential needs (e.g., nutrients and physical root space) may not be met, thus affecting biomass accumulation in organs and the whole plant (Poorter et al., 2012). To simulate the potential effects associated with sea-level rise and saltwater intrusion, some stress levels in these controlled experiments, such as flooding salinity at 35 ppt, would pose more severe threats to halophytes than conditions encountered in the field. Another potential problem was the short period of controlled experiments (about 3–4 months), which might be not sufficient to overcome the influence from the three months growth before the experiments. The simulation of tides was finished before 9 am and started after 5 pm, which could have partly affected the time of photosynthesis.

TB for all species studied in our controlled experiments were close to the values of a field investigation in the Jiuduan shoal of the Yangtze River Estuary by Liu et al. (2013), and were slightly higher than those in the Dongtan wetland by Yan et al. (2014). Comparisons were only conducted in the Yangtze River Estuary to avoid the differences in genotype and environmental conditions. In summary, the positive and negative impacts of controlled experiments slightly affected plant traits, resulting in the discrepancies of biomass accumulation between controlled experiments and other field studies. Nevertheless, these slight biases indicated that our findings were not overly influenced by the controlled experimental design, and should not affect the quantitative analyses of the responses to environmental gradients. The controlled experiments simplified the field conditions and inevitably had inherent weaknesses. However, these experiments were an essential step to understanding the complex ecological processes and investigating the potential impacts of global climate change on estuarine ecosystems, such as sea-level rise and saltwater intrusion.

Conclusion

In the present study, we highlighted the importance of salinity and inundation regimes as crucial abiotic drivers influencing the ability of halophytes to maintain soil surface elevation in estuarine salt marshes, especially under the accelerated sea-level rise and aggravated saltwater intrusion scenarios. There were significant decreases in TB of *P. australis*, *S. alterniflora*, and *S. mariqueter* with increasing flooding salinity from freshwater (0 ppt) to seawater (35 ppt). Elevated flooding depth (10–80 cm) exerted insignificant effects on TB of *P. australis* and *S. mariqueter*, but induced significant decreases in their live AGB. In contrast, the non-native *S. alterniflora* was less severely affected than the other two native species by flooding salinity, and still had high TB at a flooding depth of 80 cm, which could not only directly reflect its high tolerance to experimental conditions, but also partly explain its rapid expansion in the salt marsh of the Yangtze River Estuary. No significant differences in TB were observed in the flooding frequency treatments. Moreover, no significant variations in the BGB were detected among treatments. Elevated flooding salinity and flooding depth levels caused by rising sea-levels and saltwater intrusion might lead to significant decreases in the live AGB of halophytes, which could partly affect their ability to accumulate organic matter and trap sediments. However, as the phenotypic plasticity to stressful environmental conditions, the relatively high BGB:AGB ratios for *P. australis* and *S. mariqueter* were conducive to maintenance of marsh elevation and allowed the marsh to keep pace with rising sea-level. Relying on salt marsh species to modify the elevation of their habitat is an intriguing strategy worth further investigation. Even so, we suggest that changes in sea-level and saltwater intrusion may promote expansion of halophytes less sensitive and highly resilient, such as the non-native *S. alterniflora* in Yangtze River Estuary.

Acknowledgements This work was sponsored by the National Natural Science Foundation of China (Grant Numbers 41271065, 41371112 and 41571083), the Natural Science Foundation of Shanghai (16ZR1410300), and the National Key Research and Development Program of China (2017YFC0506000). We thank André A. Padial, the associate editor, and three anonymous reviewers for their constructive suggestions. We also greatly appreciate the efforts of Yunqing Zhang, Bin Yang, and Junyan Jiang in conducting field and laboratory work.

References

Artigas, F., J. Y. Shin, C. Hobble, A. Marti-Donati, K. V. R. Schäfer & I. Pechmann, 2015. Long term carbon storage potential and CO_2 sink strength of a restored salt marsh in New Jersey. Agricultural and Forest Meteorology 200: 313–321.

Barbier, E. B., S. D. Hacker, C. Kennedy, E. W. Koch, A. C. Stier & B. R. Silliman, 2011. The value of estuarine and coastal ecosystem services. Ecological Monographs 81: 169–193.

Baustian, J. J., I. A. Mendelssohn & M. W. Hester, 2012. Vegetation's importance in regulating surface elevation in a coastal salt marsh facing elevated rates of sea level rise. Global Change Biology 18: 3377–3382.

Brownstein, G., J. B. Wilson & D. J. Burritt, 2013. Waterlogging tolerance on a New Zealand saltmarsh. Journal of Experimental Marine Biology and Ecology 446: 202–208.

Canalejo, A., D. Martínez-Domínguez, F. Córdoba & R. Torronteras, 2014. Salt tolerance is related to a specific antioxidant response in the halophyte cordgrass, *Spartina densiflora*. Estuarine, Coastal and Shelf Science 146: 68–75.

Chambers, R. M., T. J. Mozdzer & J. C. Ambrose, 1998. Effects of salinity and sulfide on the distribution of *Phragmites australis* and *Spartina alterniflora* in a tidal saltmarsh. Aquatic Botany 62: 161–169.

Chen, Z. Y., B. Li, Y. Zhong & J. K. Chen, 2004. Local competitive effects of introduced *Spartina alterniflora* on *Scirpus mariqueter* at Dongtan of Chongming Island, the Yangtze River estuary and their potential ecological consequences. Hydrobiologia 528: 99–106.

Chmura, G. L., S. C. Anisfeld, D. R. Cahoon & J. C. Lynch, 2003. Global carbon sequestration in tidal, saline wetland soils. Global Biogeochemical Cycles 17: 1111.

Colmer, T. D. & T. J. Flowers, 2008. Flooding tolerance in halophytes. New Phytologist 179: 964–974.

Colmer, T. D., O. Pedersen, A. M. Wetson & T. J. Flowers, 2013. Oxygen dynamics in a salt-marsh soil and in *Suaeda maritima* during tidal submergence. Environmental and Experimental Botany 92: 73–82.

Darby, F. A. & R. E. Turner, 2008. Below- and aboveground *Spartina alterniflora* production in a Louisiana salt marsh. Estuaries and Coasts 31: 223–231.

Dausse, A., A. Garbutt, L. Norman, S. Papadimitriou, L. M. Jones, P. E. Robins & D. N. Thomas, 2012. Biogeochemical functioning of grazed estuarine tidal marshes along a salinity gradient. Estuarine, Coastal and Shelf Science 100: 83–92.

Davy, A. J., M. J. H. Brown, H. L. Mossman & A. Grant, 2011. Colonization of a newly developing salt marsh: disentangling independent effects of elevation and redox potential on halophytes. Journal of Ecology 99: 1350–1357.

de Klein, J. J. M. & A. K. van der Werf, 2014. Balancing carbon sequestration and GHG emissions in a constructed wetland. Ecological Engineering 66: 36–42.

Ding, W. H., J. Y. Jiang, X. Z. Li, X. Huang, X. Z. Li, Y. X. Zhou & C. D. Tang, 2015. Spatial distribution of species and influencing factors across salt marsh in southern Chongming Dongtan. Chinese Journal of Plant Ecology 39: 704–716 (in Chinese with English abstract).

Diskin, M. S. & D. L. Smee, 2017. Effects of black mangrove *Avicennia germinans* expansion on salt marsh nekton assemblages before and after a flood. Hydrobiologia. doi:10.1007/s10750-017-3179-2.

Engels, J. G., F. Rink & K. Jensen, 2011. Stress tolerance and biotic interactions determine plant zonation patterns in estuarine marshes during seedling emergence and early establishment. Journal of Ecology 99: 277–287.

Flowers, T. J. & T. D. Colmer, 2008. Salinity tolerance in halophytes. New Phytologist 179: 945–963.

Freschet, G. T., E. M. Swart & J. H. Cornelissen, 2015. Integrated plant phenotypic responses to contrasting above- and below-ground resources: key roles of specific leaf area and root mass fraction. New Phytologist 206: 1247–1260.

Funk, J. L., 2008. Differences in plasticity between invasive and native plants from a low resource environment. Journal of Ecology 96: 1162–1173.

Galvan-Ampudia, C. S. & C. Testerink, 2011. Salt stress signals shape the plant root. Current Opinion in Plant Biology 14: 296–302.

Ge, Z. M., H. Q. Guo, B. Zhao, C. Zhang, H. Peltola & L. Q. Zhang, 2016. Spatiotemporal patterns of the gross primary production in the salt marshes with rapid community change: a coupled modeling approach. Ecological Modelling 321: 110–120.

Gedan, K. B., B. R. Silliman & M. D. Bertness, 2009. Centuries of human-driven change in salt marsh ecosystems. Annual Review of Marine Science 1: 117–141.

Gillanders, B. M., T. S. Elsdon, I. A. Halliday, G. P. Jenkins, J. B. Robins & F. J. Valesini, 2011. Potential effects of climate change on Australian estuaries and fish utilising estuaries: a review. Marine and Freshwater Research 62: 1115–1131.

He, Q., B. S. Cui, Y. Z. Cai, J. F. Deng, T. Sun & Z. F. Yang, 2009. What confines an annual plant to two separate zones along coastal topographic gradients? Hydrobiologia 630: 327–340.

He, Y. L., X. Z. Li, C. Craft, Z. G. Ma & Y. G. Sun, 2011. Relationships between vegetation zonation and environmental factors in newly formed tidal marshes of the Yangtze River estuary. Wetlands Ecology and Management 19: 341–349.

Hopkinson, C. S., W. Cai & X. Hu, 2012. Carbon sequestration in wetland dominated coastal systems – a global sink of rapidly diminishing magnitude. Current Opinion in Environmental Sustainability 4: 186–194.

Hu, Y., L. Wang, Y. S. Tang, Y. L. Li, J. H. Chen, X. F. Xi, Y. N. Zhang, X. H. Fu, J. H. Wu & Y. Sun, 2014. Variability in soil microbial community and activity between coastal and riparian wetlands in the Yangtze River estuary – Potential impacts on carbon sequestration. Soil Biology and Biochemistry 70: 221–228.

Hyndes, G. A., I. Nagelkerken, R. J. McLeod, R. M. Connolly, P. S. Lavery & M. A. Vanderklift, 2014. Mechanisms and ecological role of carbon transfer within coastal seascapes. Biological Reviews 89: 232–254.

IPCC, 2013. Summary for policymakers. In Stocker, T., D. Qin, G. K. Plattner, M. Tignor, S. Allen, J. Boschung, A. Nauels, Y. Xia, V. Bex & P. Midgley (eds), Climate Change 2013: the Physical Science Basis. Contribution of Working Group I to the Fifth Assessment Report of the Intergovernmental Panel on Climate Change. Cambridge University Press, Cambridge and New York: 3–32.

Jennerjahn, T. C. & S. B. Mitchell, 2013. Pressures, stresses, shocks and trends in estuarine ecosystems – an introduction and synthesis. Estuarine, Coastal and Shelf Science 130: 1–8.

Julkowska, M. M. & C. Testerink, 2015. Tuning plant signaling and growth to survive salt. Trends in Plant Science 20: 586–594.

Kang, H., I. Jang & S. Kim, 2012. Key processes in CH_4 dynamics in wetlands and possible shifts with climate change. In Middleton, B. A. (ed.), Global Change and the Function and Distribution of Wetlands. Springer, Netherlands: 99–114.

Kathilankal, J. C., T. J. Mozdzer, J. D. Fuentes, P. D'Odorico, K. J. McGlathery & J. C. Zieman, 2008. Tidal influences on carbon assimilation by a salt marsh. Environmental Research Letters 3: 044010.

Kirwan, M. L. & G. R. Guntenspergen, 2012. Feedbacks between inundation, root production, and shoot growth in a rapidly submerging brackish marsh. Journal of Ecology 100: 764–770.

Kirwan, M. L. & J. P. Megonigal, 2013. Tidal wetland stability in the face of human impacts and sea-level rise. Nature 504: 53–60.

Kirwan, M. L. & S. M. Mudd, 2012. Response of salt-marsh carbon accumulation to climate change. Nature 489: 550–553.

Langley, J. A., T. J. Mozdzer, K. A. Shepard, S. B. Hagerty & J. P. Megonigal, 2013. Tidal marsh plant responses to elevated CO_2, nitrogen fertilization, and sea level rise. Global Change Biology 19: 1495–1503.

Lewis, D. B., J. A. Brown & K. L. Jimenez, 2014. Effects of flooding and warming on soil organic matter mineralization in *Avicennia germinans* mangrove forests and *Juncus roemerianus* salt marshes. Estuarine, Coastal and Shelf Science 139: 11–19.

Li, B., C. Z. Liao, X. D. Zhang, H. L. Chen, Q. Wang, Z. Y. Chen, X. J. Gan, J. H. Wu, B. Zhao, Z. J. Ma, X. L. Cheng, L. F. Jiang & J. K. Chen, 2009. *Spartina alterniflora* invasions in the Yangtze River estuary, China: an overview of current status and ecosystem effects. Ecological Engineering 35: 511–520.

Li, X. Z., L. J. Ren, Y. Liu, C. Craft, Ü. Mander & S. L. Yang, 2014. The impact of the change in vegetation structure on the ecological functions of salt marshes: the example of the Yangtze estuary. Regional Environmental Change 14: 623–632.

Liu, Y., X. Z. Li, Z. Z. Yan, X. Z. Chen, Y. L. He, W. Y. Guo & P. Y. Sun, 2013. Biomass and carbon storage of *Phragmites australis* and *Spartina alterniflora* in Jiuduan Shoal Wetland of Yangtze Estuary, East China. Chinese Journal of Applied Ecology 24: 2129–2134 (in Chinese with English abstract.

Luisetti, T., R. K. Turner, T. Jickells, J. Andrews, M. Elliott, M. Schaafsma, N. Beaumont, S. Malcolm, D. Burdon, C. Adams & W. Watts, 2014. Coastal zone ecosystem services: from science to values and decision making; a case study. Science of the Total Environment 493: 682–693.

Ma, Z. J., D. S. Melville, J. G. Liu, Y. Chen, H. Y. Yang, W. W. Ren, Z. W. Zhang, T. Piersma & B. Li, 2014. Rethinking China's new great wall. Science 346: 912–914.

Mcleod, E., G. L. Chmura, S. Bouillon, R. Salm, M. Bjork, C. M. Duarte, C. E. Lovelock, W. H. Schlesinger & B. R. Silliman, 2011. A blueprint for blue carbon: toward an improved understanding of the role of vegetated coastal habitats in sequestering CO_2. Frontiers in Ecology and the Environment 9: 552–560.

Medeiros, D. L., D. S. White & B. L. Howes, 2013. Replacement of *Phragmites australis* by *Spartina alterniflora*: the role of competition and salinity. Wetlands 33: 421–430.

Melton, J. R., R. Wania, E. L. Hodson, B. Poulter, B. Ringeval, R. Spahni, T. Bohn, C. A. Avis, D. J. Beerling, G. Chen, A. V. Eliseev, S. N. Denisov, P. O. Hopcroft, D. P. Lettenmaier, W. J. Riley, J. S. Singarayer, Z. M. Subin, H. Tian, S. Zürcher, V. Brovkin, P. M. van Bodegom, T. Kleinen, Z. C. Yu & J. O. Kaplan, 2012. Present state of global wetland extent and wetland methane modelling: conclusions from a model intercomparison project (WETCHIMP). Biogeosciences Discussions 9: 11577–11654.

Moriuchi, K. S. & A. A. Winn, 2004. Relationships among growth, development and plastic response to environment quality in a perennial plant. New Phytologist 166: 149–158.

Morris, J. T., 2007. Ecological engineering in intertidial saltmarshes. Hydrobiologia 577: 161–168.

Morris, J. T., P. V. Sundareshwar, C. T. Nietch, B. Kjerfve & D. R. Cahoon, 2002. Responses of coastal wetlands to rising sea level. Ecology 83: 2869–2877.

Morris, J. T., K. Sundberg & C. S. Hopkinson, 2013. Salt marsh primary production and its responses to relative sea level and nutrients in estuaries at Plum Island, Massachusetts, and North Inlet, South Carolina, USA. Oceanography 26: 78–84.

Mudd, S. M., A. D'Alpaos & J. T. Morris, 2010. How does vegetation affect sedimentation on tidal marshes? Investigating particle capture and hydrodynamic controls on biologically mediated sedimentation. Journal of Geophysical Research-Atmospheres 115: F03029.

Mueller, P., K. Jensen & J. P. Megonigal, 2016. Plants mediate soil organic matter decomposition in response to sea level rise. Global Change Biology 22: 404–414.

Munns, R. & M. Tester, 2008. Mechanisms of salinity tolerance. Annual Review of Plant Biology 59: 651–681.

Negrin, V. L., A. E. de Villalobos, G. Gonzalez Trilla, S. E. Botte & J. E. Marcovecchio, 2012. Above- and belowground biomass and nutrient pools of *Spartina alterniflora* (smooth cordgrass) in a South American salt marsh. Chemistry and Ecology 28: 391–404.

Niklas, K. J. & B. J. Enquist, 2002. On the vegetative biomass partitioning of seed plant leaves, stems, and roots. American Naturalist 159: 482–497.

Onkware, A. O., 2000. Effect of soil salinity on plant distribution and production at Loburu Delta, Lake Bogoria National Reserve, Kenya. Austral Ecology 25: 140–149.

Osland, M. J., N. M. Enwright, R. H. Day, C. A. Gabler, C. L. Stagg & J. B. Grace, 2016. Beyond just sea-level rise: considering macroclimatic drivers within coastal wetland vulnerability assessments to climate change. Global Change Biology 22: 1–11.

Pendleton, L., D. C. Donato, B. C. Murray, S. Crooks, W. A. Jenkins, S. Sifleet, C. Craft, J. W. Fourqurean, J. B. Kauffman, N. Marba, P. Megonigal, E. Pidgeon, D. Herr, D. Gordon & A. Baldera, 2012. Estimating global "blue carbon" emissions from conversion and degradation of vegetated coastal ecosystems. PLoS ONE 7: e43542.

Pennings, S. C., M. B. Grant & M. D. Bertness, 2005. Plant zonation in low-latitude salt marshes: disentangling the roles of flooding, salinity and competition. Journal of Ecology 93: 159–167.

Pfennig, D. W., M. A. Wund, E. C. Snell-Rood, T. Cruickshank, C. D. Schlichting & A. P. Moczek, 2010. Phenotypic plasticity's impacts on diversification and speciation. Trends in Ecology & Evolution 25: 459–467.

Poffenbarger, H. J., B. A. Needelman & J. P. Megonigal, 2011. Salinity influence on methane emissions from tidal marshes. Wetlands 31: 831–842.

Poorter, H., K. J. Niklas, P. B. Reich, J. Oleksyn, P. Poot & L. Mommer, 2012. Biomass allocation to leaves, stems and roots: meta-analyses of interspecific variation and environmental control. New Phytologist 193: 30–50.

Regnier, P., P. Friedlingstein, P. Ciais, F. T. Mackenzie, N. Gruber, I. A. Janssens, G. G. Laruelle, R. Lauerwald, S. Luyssaert, A. J. Andersson, S. Arndt, C. Arnosti, A. V. Borges, A. W. Dale, A. Gallego-Sala, Y. Goddéris, N. Goossens, J. Hartmann, C. Heinze, T. Ilyina, F. Joos, D. E. LaRowe, J. Leifeld, F. J. R. Meysman, G. Munhoven, P. A. Raymond, R. Spahni, P. Suntharalingam & M. Thullner, 2013. Anthropogenic perturbation of the carbon fluxes from land to ocean. Nature Geoscience 6: 597–607.

Scarton, F., J. W. Day & A. Rismondo, 2002. Primary production and decomposition of *Sarcocornia fruticosa* (L.) Scott and *Phragmites australis* Trin. ex Steudel in the Po Delta, Italy. Estuaries and Coasts 25: 325–336.

Shelford, V. E., 1931. Some concepts of bioecology. Ecology 12: 455–467.

Silvestri, S., A. Defina & M. Marani, 2005. Tidal regime, salinity and salt marsh plant zonation. Estuarine, Coastal and Shelf Science 62: 119–130.

Snedden, G. A., K. Cretini & B. Patton, 2015. Inundation and salinity impacts to above- and belowground productivity in *Spartina patens* and *Spartina alterniflora* in the Mississippi River deltaic plain: Implications for using river diversions as restoration tools. Ecological Engineering 81: 133–139.

SOA (State Oceanic Administration People's Republic of China), 2015. China sea-level communique. http://www.coi.gov.cn/gongbao/haipingmian/201503/t20150326_32297.html Accessed July 5, 2016.

SOA (State Oceanic Administration People's Republic of China), 2016. China sea-level communique. http://www.coi.gov.cn/gongbao/haipingmian/201603/t20160328_33812.html Accessed July 5, 2016.

Sousa, A. I., A. I. Lillebø, M. A. Pardal & I. Caçador, 2010a. Productivity and nutrient cycling in salt marshes: contribution to ecosystem health. Estuarine, Coastal and Shelf Science 87: 640–646.

Sousa, A. I., A. I. Lillebø, M. A. Pardal & I. Caçador, 2010b. The influence of *Spartina maritima* on carbon retention capacity in salt marshes from warm-temperate estuaries. Marine Pollution Bulletin 61: 215–223.

Spalding, E. A. & M. W. Hester, 2007. Interactive effects of hydrology and salinity on oligohaline plant species productivity: implications of relative sea-level rise. Estuaries and Coasts 30: 214–225.

Steinman, A. D., M. E. Ogdahl, M. Weinert & D. G. Uzarski, 2014. Influence of water-level fluctuation duration and magnitude on sediment-water nutrient exchange in coastal wetlands. Aquatic Ecology 48: 143–159.

Sutter, L. A., R. M. Chambers & J. E. Perry, 2015. Seawater intrusion mediates species transition in low salinity, tidal marsh vegetation. Aquatic Botany 122: 32–39.

Tang, L., Y. Gao, B. Li, Q. Wang, C. H. Wang & B. Zhao, 2014. *Spartina alterniflora* with high tolerance to salt stress changes vegetation pattern by outcompeting native species. Ecosphere 5: 116.

Theuerkauf, E. J., J. D. Stephens, J. T. Ridge, F. J. Fodrie & A. B. Rodriguez, 2015. Carbon export from fringing saltmarsh shoreline erosion overwhelms carbon storage across a critical width threshold. Estuarine, Coastal and Shelf Science 164: 367–378.

Wang, C. H., M. Lu, B. Yang, Q. Yang, X. D. Zhang, T. Hara & B. Li, 2010. Effects of environmental gradients on the performances of four dominant plants in a Chinese saltmarsh: implications for plant zonation. Ecological Research 25: 347–358.

Wang, Q., C. H. Wang, B. Zhao, Z. J. Ma, Y. Q. Luo, J. K. Chen & B. Li, 2006. Effects of growing conditions on the growth of and interactions between salt marsh plants: implications for invasibility of habitats. Biological Invasions 8: 1547–1560.

Yan, G., Z. M. Ge & L. Q. Zhang, 2014. Distribution of soil carbon storage in different saltmarsh plant communities in Chongming Dongtan wetland. Chinese Journal of Applied Ecology 25: 85–91 (in Chinese with English abstract).